International Journal of Latest Research in Science and Technology **ISSN (Online):2278-5299**
Volume 8, Issue 6: Page No. 1 - 11, November-December 2019
https://www.mnkjournals.com/journal/ijlrst/index.php

NEW DESIGN AND MODELIZATION OF A CONVEX GRATING FOR AN HYPERSPECTRAL IMAGER OF THE CHANDRAYAAN 2 INSTRUMENT FOR THE MOON PROBE IN THE INFRARED

Bernard Sabushimike[1*], Georges Horugavye[1], Serge Habraken[1], Jean François Jamoye[2], Vincent Moreau[2]
[1] Holography and Optical laboratory (HOLOLAB), University of Liège, Belgium
[2] AMOS, Liège Science Park, 2 Rue des Chasseurs Ardennais, B-4031 ANGLEUR, Belgium,
bsabushimike@doct.ulg.ac.be, ghorugavye@doct.ulg.ac.be, shabraken@uliege.be, jfj@amos.be, vincent.moreau@amos.be

Received : 08 November 2019; **Accepted** : 28 November 2019 ; **Published** :31 December 2019

Abstract: **For hyperspectral imaging, diffraction gratings based spectrometers exhibit high spectral resolution and optical performance. Among those spectrometers, the Offner type (which consists of an entrance slit, two concave mirrors and convex grating) offers a lot of advantages. In this paper, we propose the design and modelization of a convex grating which covers a spectral band ranging from 0.7 µm to 5 µm with a minimum diffraction efficiency of 20% at 800 nm, 50% at 3000 nm and 25% at 5000 nm. For a so wide band, a grating with a single blaze cannot satisfy these requirements. We will therefore propose an approach of multi-blaze grating which is subdivided into different sections each with its own blaze angle. On April 30, 2016 we published a similar article in your journal and the optimization process resulted in a grating design of 9 blaze wavelengths. We have continued to work on this and currently we propose a better optimization method which allows to obtain the same results but only with 3 blaze wavelengths. Meanwhile, we perform the diffraction efficiency prediction using the scalar and rigorous theories to prove the compliance of this design with the technical specifications. The rigorous theory will also allow us to study the polarization sensitivity of this grating and the calculation of the diffraction efficiency of a grating with a profile degraded by manufacturing errors to assess the impact on the diffraction efficiency and the sensitivity to polarization.**

Keywords **–** Offner spectrometer, grating, blazing, multi-blaze grating

I. INTRODUCTION

Hyperspectral remote sensing has been defined as "the field of study associated with extracting information about an object without coming into physical contact with it"[1]. It combines two sensing modalities: imaging and spectrometry. An imaging system captures a picture of a remote scene related to the spatial distribution of the power of reflected and/or emitted electromagnetic radiation integrated over some spectral band. On the other hand, spectrometry measures the variation in power with the wavelength or frequency of light, capturing information related to the chemical composition of the materials measured[2]. Our study focuses on this second part proposing an optimization method of a convex grating for the hyperspectral imager spectrometer of the Chandrayaan 2[3] instrument which covers a spectral range from 0.7 µm to 5 µm with diffraction efficiency described in section V. In this manuscript, we return to the previous version of the article already published[4] to apply a new optimization method for a multi-blaze grating. For spectrometry, an optical system with convex grating in Offner configuration demonstrates a high performance with a compact volume.

II. CONVEX GRATING SPECTROMETER IN OFFNER CONFIGURATION

An Offner grating spectrometer design requires the use of convex blazed grating that can be produced by ruling or diamond turning. It consists of a slit, two concave mirrors and a diffraction convex grating between them. Because of the asymmetry introduced by grating diffraction, a split-Offner design is employed, where orientation of the two mirrors is slightly asymmetric. This configuration offers a larger field of view and lower aberrations. These spectrometers have a concentric structure and thus a compact design. They operate with a relatively low F-number (≤f/2), accept a long slit while maintaining a compact size, and need only three optical surfaces. The use of this design has resulted in imaging spectrometers with extremely low values of spatial-spectral distortion[5]. Most land observation hyperspectral instruments are based on Offner configuration. This is the case of the Hyperion instrument on board EO-1 NASA platform or HyspIR[6], but also for the imaging spectrometer for planetary mineralogy[7], EnMAP[8], CHRIS (on board proba-1)[9].

The present instrument (Chandrayaan 2) consists of a four optics telescope, slit, spectrometer, order sorting filter and detector. The instrument design is presented at figure 1

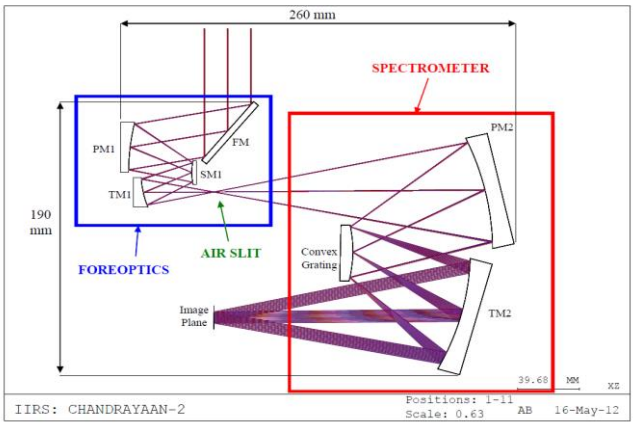

Fig. 1: Hyperspectral instrument design (AMOS proprietary).

III. DIFFRACTION GRATING EQUATION

When a diffraction grating is illuminated with a beam of monochromatic light, the diffraction orders, in reflection and/or in transmission, are governed by the so-called equation of the diffraction gratings represented by the equation (1). This manuscript will focus on reflective gratings. For grating period Λ, the incident beam of a wavelength λ illuminating the grating with an angle of incidence θ_i with respect to the normal at the incidence point on the grating, will be diffracted in discrete diffraction orders m (m is a relative integer) with an angle θ_d given by:

$$\Lambda(\sin\theta_i + \sin\theta_d) = m\lambda \qquad (1)$$

This equation is valid in reflection and transmission provided that the diffraction angle is positively counted if it is located on the same side as the angle of incidence with respect to the normal and negatively otherwise[10]

IV. GRATING DESCRIPTION

The grating description is summarized in the table 1.

Table 1: grating specification related to Chandrayaan 2 mission [3]

Surface profile	Convex spherical
Surface shape	Circular
Clear aperture	>37 mm
Radius curvature	88.4±0.05 mm
Material	Optical grade aluminium
Coating	Gold
Groove density	20 grooves/mm
Incidence angle of the central field	27.12 degrees
Optimization order	+1

V. DESIGN AND MODELIZATION OF THE CONVEX GRATING

A. INTRODUCTION

The grating specifications require a period of 50 µm with a spectral range of operation from 0.7 to 5µm. Based on a preliminary study, we understand the challenge due to the wide spectral bandwidth. As a consequence, a multi-blaze grating is predicted as the only viable solution. The choice of blaze angles and the configuration are dictated by the required diffraction efficiency defined by figure 2.

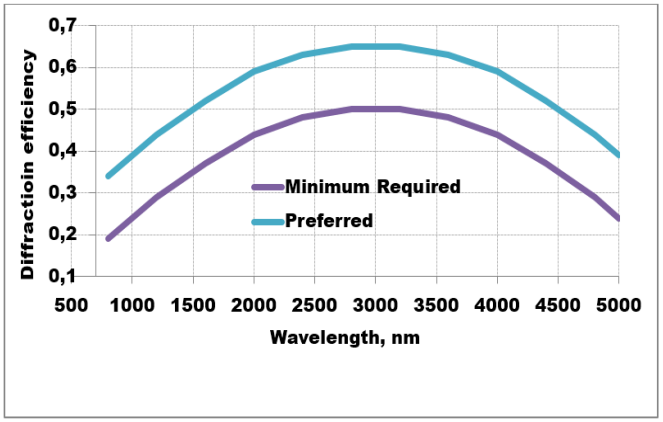

Fig. 2: Diffraction efficiency requirement for the convex grating.

As far as modelling of surface-relief metallic gratings is concerned, an efficient tool is the *PCGrate* software based on a rigorous integral method of solving the electromagnetic problem[11]. Blazed gratings with TE and TM polarization on flat or non-flat substrate can be modeled and optimized. The diffraction efficiency over the diffraction orders is fully characterized. Numerical instabilities can arise, especially with large period as we find in this case.

For that reason, a simpler more intuitive approach is also possible since the grating period is large, compared to the wavelength: the "scalar theory" approach is another useful tool. Both tools will be used and compared to enhance the trust level of simulations. However, only the rigorous theory will give information about the polarization sensitivity of the grating.

This paper will focus on the optimization of the Chandrayaan 2 diffraction grating. The goal is to fulfill the requirements, especially the spectral behavior of the diffraction efficiency and the polarization sensitivity. The proposed method consists in defining a "multi-blazed profile" and we will use both scalar and rigorous theories.

B. Scalar theory

The scalar theory is very convenient. It is a theory that ignores the vectorial aspect of light but provides results comparable with those obtained with rigorous theories under specific conditions while being less time consuming and easier to implement. Moreover, the scalar theory allows for an easier approach to optimize diffraction gratings, while rigorous theories sound more like tools to check the diffraction characteristics for the gratings designed. The scalar theory is a powerful tool to deal with high period to wavelength ratio grating. Scalar theory is known to be accurate if [12], [13]

$$\frac{\Lambda}{\lambda} \geq 10 \qquad (2)$$

Where Λ is the grating period and λ is the wavelength.

For the Chandrayaan 2 hyperspectral imaging spectrometer, the wavelength range extents from 0.7 to 5µm for a grating period of 50µm. Even the worst case (50µm/5µm) responds to the scalar theory criterion. This means that Fourier theory can be used. However, this model does not take into account the polarization state. The scalar diffraction efficiency for reflective gratings assuming a perfect reflective coating is given by[14]:

$$\eta_{dif} = sinc^2\left(\frac{2h}{\lambda} - k\right) \quad (3)$$

Where k is the diffraction order and *h* is the grating thickness directly linked to the blazed wavelength:

$$\lambda_b = \frac{2h}{k} \quad (4)$$

Therefore, for one given thickness when $\lambda = \lambda_b$, the grating achieves 100% diffraction efficiency at the diffraction order k. The diffraction efficiency will be zero for every other diffraction orders. Combining equations 3 and 4, the diffraction efficiency for the first order (k = +1) of diffraction becomes:

$$\eta_{dif} = sinc^2\left(\frac{\lambda_b}{\lambda} - 1\right) \quad (5)$$

C. Rigorous theory: "PCGrate software"

Our rigorous analysis tool allows calculating the diffraction efficiency of gratings on plane, spherical, cylindrical and aspherical surfaces. *PCGrate* uses an accurate boundary integral equation method, with some optimization parameters, which is described with numerous references directly on the website of *PCGrate*[15].

D. Optimization of the grating profile

The optimization of the grating profiles depend on the technical characteristics of the grating, namely, the requirements in terms of diffraction efficiency, spectral bandwidth, optimization order, etc. In addition to the classical single-blaze grating, we present a multi-blaze grating approach.

1. Single-blaze grating

A single-blaze grating is a mono angle blazed grating and therefore with a uniform profile over its entire surface. The optimization of this grating is very simple and is done using the diffraction gratings equation (1). Figure 3 shows an example of single-blaze grating where Λ, α, and h are, respectively, period, blaze angle, and groove depth. Once the optimization is complete, that is to say, when all the grating parameters are known, the calculation of the grating diffraction efficiency is done by the scalar and/or rigorous theories.

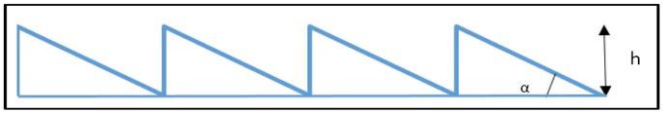

Fig. 3: Example of a single-blaze grating.

2. Multiblaze grating

In 1998, Mouroulis et al. proposed a grating design based on multiblaze profiles[16]. Such a design aims to meet the requirements of the grating in terms of diffraction efficiency, which a single blaze cannot satisfy, over a well-defined spectral band. Figure 4 shows an example of multi-blaze grating. The number of blaze wavelengths and their values depend on the grating technical specifications. The goal of this paper is to propose an optimization method that allows one to find the number of blaze wavelengths of the grating, their values and their weights to meet the diffraction efficiency requirements. The proposed method will use the diffractive scalar theory to calculate the grating diffraction efficiency and others optimization tools.

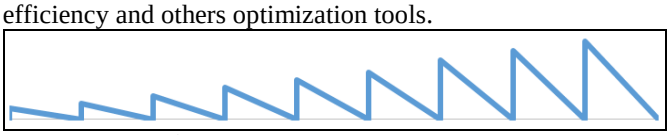

Fig. 4: Example of multiblaze grating. The period remains constant.The blaze angle is variable, and the groove depth is adapted.

The multiblaze gratings can be defined over a period [13], [17], [18], [19] but in our case, the hybrid grating profile might be built as an ensemble of sub-gratings (sections) each with its blaze angle at fix period and fix draft angle α (often assumed as zero). It means that the groove depth h is increasing when the blazing angle ϒ increases as shown on figure 5.

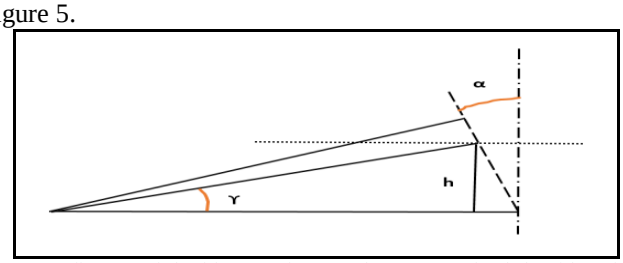

Fig. 5: Influence of the blaze angle γ on the grooves depth h with a draft angle α.

During the manufacture of the multi-blaze grating, it is obligatory to change the slope of the diamond cutting tool to change the blaze angle and the depth passing from one section to the other. In this case, the rulings between different blazes will tend to match at the peaks and the difference between the average heights will be high. Therefore the mean phase difference is considerably large[16]. This would have a detrimental effect on the point spread function (PSF). The ideal solution is to match the mean heights thus leading to a zero mean phase difference between the blazes.

E. Optimization tools

1. Function fsolve

We are going to apply a new method[20] to optimize a multi-blaze grating based on the fsolve function of which we present a summary in the following lines. The function fsolve[21] is a MATLAB optimization tool and is used to solve a system of nonlinear equations:

$$x = f\,solve\,(@functionname, x0, options) \quad (6)$$

Input arguments

The first argument functionname is thename of the system of nonlinear equations to solve. Functionname is a function

that accepts a vector x and returns a vector F, the nonlinear equations evaluated at x. The functionname can be specified as an M-file function. It is a MATLAB function such that functionname has to match the file name. A function file is not executable by itself; it can only be called in other commands. It is defined by the following equation:

$$\begin{cases} \text{Function F} = \text{functionname(x)} \\ \text{F} = \text{Expression of the system} \end{cases} \quad (7)$$

The second argument x0 is the arbitrary initial vector for x. It is a vector whose components are wavelengths and their weights. The number of those components is equal to the number of unknowns to be determined. The third argument options is the options structure created with the optimoptions tool. Optimoptions allows to create or edit optimization options structure:
Options = optimoptions ('param1', value1,'param2', value2,...) creates an optimization option structure called options, in which the specified options (param) have specified values. fsolve uses large scale and medium scale algorithms. Some options apply to both algorithms, some are only relevant when using the large-scale algorithm, and others are only relevant when using the medium-scale algorithm. In this manuscript, the options structure will allow to define the algorithm that the fsolve function uses to solve the system of nonlinear equations and give the desired blaze wavelengths.

2. *Algorithms*

By default fsolve chooses the medium-scale algorithm based on the nonlinear least-squares algorithms and uses the trust-region dogleg method[22]. This method is an iterative procedures in which the objective function is represented by a quadratic model inside a suitable neighborhood (the trust region) of the current iterate, as implied by the Taylor series expansion. This method can only be used when the system of equations is square, i.e., the number of equations equals the number of unknowns. The medium-scale algorithm uses two other methods for which the system of equations need not be square:
1.The Gauss-Newton method is a method for minimizing a sum-of-squares objective function. It presumes that the objective function is approximately quadratic in the parameters near the optimal solution[22].
2.The Levenberg-Marquardt method is a standard technique for solving nonlinear least squares problems. This method is a combination of two methods: the gradient descent method and the Gauss-Newton method[23].
The second algorithm used by the function fsolve is the large-scale algorithm which is a subspace trust-region method and is based on the interior-reflective Newton method[24],[25]. The LargeScale option specifies a preference for which algorithm to use. It is only a preference because certain conditions must be met to use the large-scale algorithm. For this algorithm, the nonlinear system of equations cannot be underdetermined; that is, the number of equations (the number of elements of F returned by functionname) must be at least as many as the number of unknowns or else the medium-scale algorithm is used.

In this manuscript, the system of nonlinear equations used to determine the blaze wavelengths is not necessary square and also each equation of the system is not quadratic. Then, the most appropriate method to solve this system is the Levenberg-Marquardt algorithm. This algorithm is suitable even if the system may not have a zero. The algorithm still returns a point where the residual is small. The idea is to construct systems of m (constant) equations with n variables, n varying from 1 (mono-blaze) to N. Here N represents the minimum number of blaze wavelengths and their weights that will result from the optimization.

F. Determination of the best grating configuration by the optimization method of the previous section

We will first determine some values of diffraction efficiency η on the desired reference curve in the figure 6. The objective is to have a grating configuration with a diffraction efficiency curve that can fitter the desired efficiency curve.
1. η (λ=700 nm) =0.31
2. η (λ =1100 nm) =0.42
3. η (λ =1500 nm) =0.50
4. η (λ =2000 nm) =0.59
5. η (λ =2500 nm) =0.64
6. η (λ =3000 nm) =0.655
7. η (λ =3500 nm) =0.64
8. η (λ =4000 nm) =0.59
9. η (λ =4500 nm) =0.50
10. η (λ =5000 nm) =0.39

The figure 6 shows the reference curves and the values selected on the desired curve. These values will be used to define the systems of equations to be used to determine blaze wavelengths, their values and their weights. Ten diffraction efficiency values are defined, which means that the systems will have 10 equations each with n variables, n varying from n = 1 (mono-blaze grating) to n = N (multi-blaze grating), N being the minimum number of blaze wavelengths and their weights that will result from the optimization process. The ten values of diffraction efficiency selected are represented by the ten red dots in Figure 6.

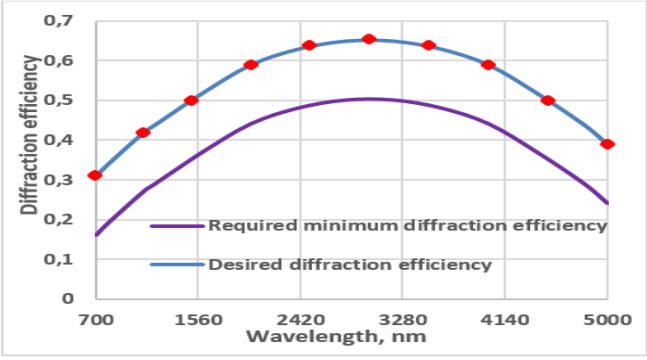

Fig. 6: Required diffraction efficiency for the convex grating with the ten values selected on the curve that will be used to determine blaze wavelengths.

1. *Mono-blaze solution*

Even if we know that a grating optimized at a single blaze wavelength is not suitable for this problem, for reason of methodology we begin to look for the best mono-blaze solution to this problem. The function F which defines the

system of nonlinear equations for N = 1 (mono-blaze grating) is given by the the “systeme1bis”. In this system,

```
function F=systeme1bis(x)
F=[(sin(pi*((x(1)/700)-1))/(pi*((x(1)/700)-1)))^2-0.31;
   (sin(pi*((x(1)/1100)-1))/(pi*((x(1)/1100)-1)))^2-0.42;
   (sin(pi*((x(1)/1500)-1))/(pi*((x(1)/1500)-1)))^2-0.50;
   (sin(pi*((x(1)/2000)-1))/(pi*((x(1)/2000)-1)))^2-0.59;
   (sin(pi*((x(1)/2500)-1))/(pi*((x(1)/2500)-1)))^2-0.64;
   (sin(pi*((x(1)/3000)-1))/(pi*((x(1)/3000)-1)))^2-0.655;
   (sin(pi*((x(1)/3500)-1))/(pi*((x(1)/3500)-1)))^2-0.64;
   (sin(pi*((x(1)/4000)-1))/(pi*((x(1)/4000)-1)))^2-0.59;
   (sin(pi*((x(1)/4500)-1))/(pi*((x(1)/4500)-1)))^2-0.50;
   (sin(pi*((x(1)/5000)-1))/(pi*((x(1)/5000)-1)))^2-0.39];
```

each equation of the system defines the value of the diffraction efficiency required for a given wavelength using scalar diffraction theory.
x (1) represents the blaze wavelength to determine for the mono-blaze grating. Does this blaze wavelength exist to meet the requirements of the grating? We intuitively know that the answer is no. This system must be solved using the Levenberg-Marquardt algorithm. It is a numerical analysis algorithm used to solve a system of nonlinear problems. Currently, this method is implemented in Matlab by the fsolve function whose syntax is given by the equation (8) and the rest is explained with the MatLab routine as an illustration of the principle. The mathematical developments of this algorithm are detailed in the articles cited in reference for interested readers.

$$\begin{cases} x0 = p; \\ Options = optimoptions(@fsolve,'Algorithm', \\ \qquad\qquad ,'levenberg-marquardt'); \\ x = fsolve(@systeme1, x0, options) \end{cases} \quad (8)$$

In this code, x0 is the arbitrary initial vector with only one component p because there is one blaze wavelength (one variable) to be determined. The options are defined by the "optimoptions" tool which has in this case two arguments: the first indicates the solver used, the second and the third its method (Levenberg-Marquardt). Finally, the function "fsolve" gives the solution of the system. It has three arguments: the first one is a function handle (@ plus the name of the file corresponding to the system) which is a Matlab value that provides a means of calling a function indirectly, the second argument corresponds to the initial vector and the third calls the defined options.

For this system, the best estimate of the solution of the system by equation (8) gives a blaze wavelength of 2277 nm for any initial vector X0. This estimate is certainly not a root of the system, but gives a blaze wavelength that produces a diffraction efficiency as close as possible to that required for a mono-blaze grating.

Profile construction

Using the rigorous theory, we simulated the grating performance with respect to the grating profile, starting from the ideal triangular blaze profile. We know that tooling can produce manufacturing defects. We consider a profile whose top is flattened on 5 µm and the bottom of the grooves rounded with a radius of curvature of 5 (10) µm on the last 3 (5) microns for the grooves less (more) rounded.

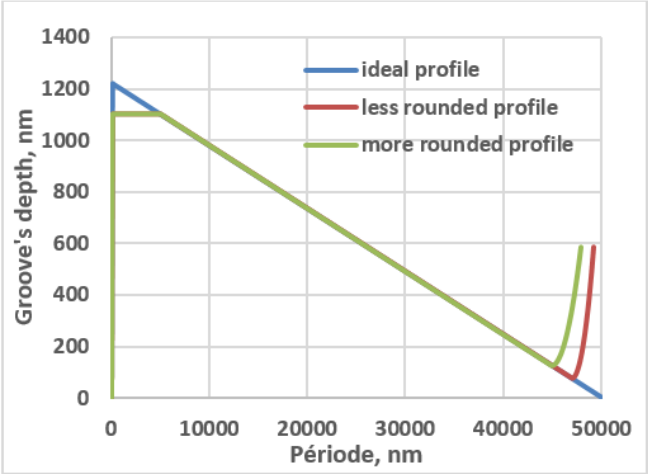

Fig. 7: Ideal and rounded profiles used in simulations for a blaze wavelength of 2277 nm (the axes are not at the same scale).

The diffraction efficiency of the mono-blaze grating with this blaze wavelength calculated using the scalar theory is given by Figure 8.

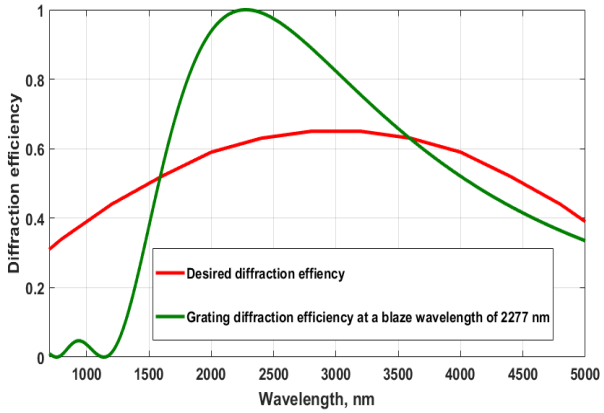

Fig. 8: First-order diffraction efficiency, for an optimized grating at single-blaze wavelength of 2277 nm, obtained by scalar theory using the ideal profile.

The area below the desired diffraction efficiency curve is 2360 AU (arbitrary unit). This surface will remain unchanged during the process of optimization of this problem. The simulation curve of the mono-blaze grating is lower than the desired curve on 55% of the spectral band. This represents a surface deficit of 366 AU in this band, which corresponds to a relative difference deficit of 15.51%. On the other hand, the simulation curve is greater than the one desired for the remaining 45% of the spectral band with a surface surplus of 448 AU, which represents a surplus in relative difference of 18.98%. These surfaces are determined using the trapezoidal method. The goal is to have a 100% curve in line with the desired reference curve. This means that the area between the desired curve and the one resulting from the optimization process must be as close as possible to zero without any deficit and surplus over the entire spectral band. Table 2

summarizes the position of the simulation curve compared to that of reference.

Table 2: Blaze wavelength and position of the simulation curve with respect to that reference according to the x0 component for N = 1.

Component of x0	Blaze wavelength	Position of the simulation curve with respect to the desired curve		
		conformity on the spectral band	Relative difference deficit on 55% of the spectral band	Relative difference surplus on 45% of the spectral band
900 nm	2277 nm	no conform	15.51%	18.98%

This solution does not meet the requirements of diffraction efficiency of the grating over the entire spectral band because the simulation curve is too far from the reference curve in the spectral band. The mono-blaze grating is not suitable for this case. Even if this mono-blaze solution is not suitable for this problem, let us compare the spectral behavior of computed diffraction efficiency with the scalar and rigorous theories at a blaze wavelength of 2277 nm. Figure 8 describes performance against an ideal profile for scalar theory, while Figure 9 shows the unpolarized diffraction efficiencies given by the rigorous theory for a grating in perfect reflection with the ideal and realistic profiles built on figures 7. As can be seen in Figures 8 and 9, the results of the scalar theory is similar to that of the rigorous theory for the ideal profile. If we compare the ideal and realistic profiles (Figure 9), the maximum diffraction efficiency has decreased by 16% from the ideal profile to the more rounded profile, with a slight shift at low wavelengths and decreases by 9% with shifting to low wavelengths going from the ideal profile to the less rounded profile. These impacts on diffraction efficiency are not negligible and must be taken into consideration by the manufacturers of the diffraction gratings. We will return to the impact of these realistic profiles on diffraction efficiency and polarization sensitivity with the best multi-blaze solution for this problem.

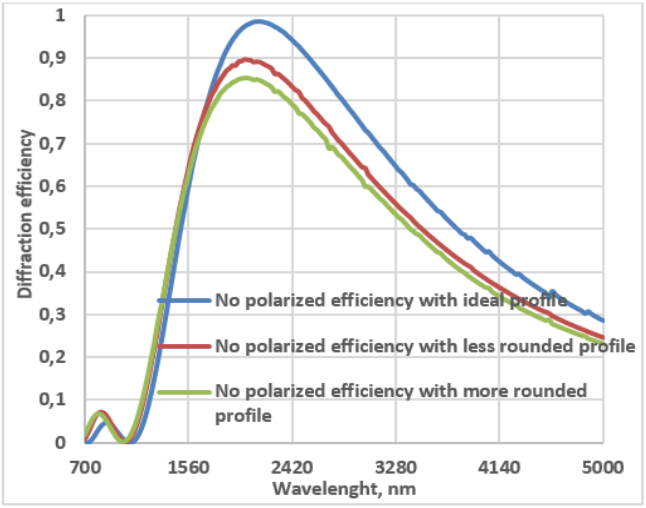

Fig. 9: First order unpolarized diffraction efficiencies for a perfect reflection grating with a single blaze 2277 nm, based on rigorous theory using ideal and realistic profiles.

2. *Solution with dual blaze wavelengths*

Based on the above results, a single wavelength blaze grating cannot meet the requirements of the grating in terms of diffraction efficiency. In this section, we investigate whether a double blaze wavelength grating can be sufficient to meet the requirements for diffraction efficiency. The system defined by the function F will be a system with four variables: two blaze wavelengths x (1) and x (2) and their weight x (3) and x (4), that is to say their contributions to the diffraction efficiency of the grating. This Function is named "syteme2bis". The solution will be valid if each weight is positive and the sum of the weights is equal to 1. In practice, the weighting factor will correspond to a proportional surface area of the complete grating.

In this system, four variables are to be determined using the Levenberg-Marquardt algorithm, as described in Equation (8), and the initial vector x0 will have four components. For any initial vector x0, the system admits a single solution (1541; 3160; 0.5; 0.5) that is to say two blaze wavelengths 1541 nm and 3160 nm as well as their weight 0.5 each. The diffraction efficiency of the grating corresponding to these two blaze wavelengths calculated using scalar theory is given in Figure 10 in comparison with the desired diffraction efficiency.

```
function F=systeme2bis(x)
F=[((sin(pi*((x(1)/700)-1))/(pi*((x(1)/700)-1)))^2)*x(3)+((sin(pi*((x(2)/700)-1))/(pi*((x(2)/700)-1)))^2)*x(4)-0.31;
   ((sin(pi*((x(1)/1100)-1))/(pi*((x(1)/1100)-1)))^2)*x(3)+((sin(pi*((x(2)/1100)-1))/(pi*((x(2)/1100)-1)))^2)*x(4)-0.42;
   ((sin(pi*((x(1)/1500)-1))/(pi*((x(1)/1500)-1)))^2)*x(3)+((sin(pi*((x(2)/1500)-1))/(pi*((x(2)/1500)-1)))^2)*x(4)-0.50;
   ((sin(pi*((x(1)/2000)-1))/(pi*((x(1)/2000)-1)))^2)*x(3)+((sin(pi*((x(2)/2000)-1))/(pi*((x(2)/2000)-1)))^2)*x(4)-0.59;
   ((sin(pi*((x(1)/2500)-1))/(pi*((x(1)/2500)-1)))^2)*x(3)+((sin(pi*((x(2)/2500)-1))/(pi*((x(2)/2500)-1)))^2)*x(4)-0.64
   ((sin(pi*((x(1)/3000)-1))/(pi*((x(1)/3000)-1)))^2)*x(3)+((sin(pi*((x(2)/3000)-1))/(pi*((x(2)/3000)-1)))^2)*x(4)-0.655;
   ((sin(pi*((x(1)/3500)-1))/(pi*((x(1)/3500)-1)))^2)*x(3)+((sin(pi*((x(2)/3500)-1))/(pi*((x(2)/3500)-1)))^2)*x(4)-0.64;
   ((sin(pi*((x(1)/4000)-1))/(pi*((x(1)/4000)-1)))^2)*x(3)+((sin(pi*((x(2)/4000)-1))/(pi*((x(2)/4000)-1)))^2)*x(4)-0.59;
   ((sin(pi*((x(1)/4500)-1))/(pi*((x(1)/4500)-1)))^2)*x(3)+((sin(pi*((x(2)/4500)-1))/(pi*((x(2)/4500)-1)))^2)*x(4)-0.50;
   ((sin(pi*((x(1)/5000)-1))/(pi*((x(1)/5000)-1)))^2)*x(3)+((sin(pi*((x(2)/5000)-1))/(pi*((x(2)/5000)-1)))^2)*x(4)-0.39;
     abs(x(3));
     abs(x(4));
     x(3)+x(4)-1];
```

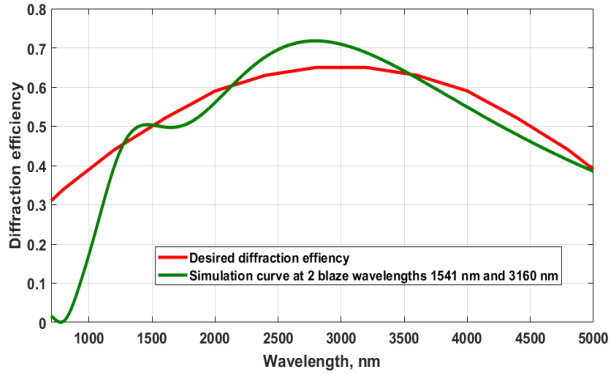

Fig.10: First order diffraction efficiency for an optimized grating at 2 blaze wavelength 1541 nm and 3160 nm obtained by scalar theory using the ideal profile.

The simulation curve of the dual-blaze grating is lower than the desired curve on 61.63% of the spectral band. This represents a surface deficit of 159 AU, which corresponds to a relative difference deficit of 6.73%. Also the simulation curve is higher than the desired reference curve on 38.37% with a superficial surplus of 93 AU, which corresponds to a relative difference surplus of 3.94%. The simulation curve corresponding to the dual-blaze grating is not consistent with the reference curve as shown in Figure 10, which means that the problem cannot be solved by this grating.

3. Grating solution with three blaze wavelengths

The previous results show that a two blaze solution is not suitable for this problem. We will build a system of equations similar to the one built in the previous subsection. Since we have three blaze wavelengths to determine and their weights, the system will have six unknowns, namely three blaze wavelengths x (1), x (2), x (3) and their respective weights x (4), x (5) and x (6). The solutions will be valid if the weights are positive and their sum equal to one. As for other cases, the system is solved using Equation (8). The initial vector x0 will have six components as the system has six unknowns.
For any initial vector x0, the system admits a unique solution, for example for x0 = [800; 900; 1000; 0.2; 0.3; 0.4], the system has for solution x = [996; 2179; 3397, 0.34, 0.33, 0.33] that is to say three blaze wavelengths 996 nm, 2179 nm and 3397 nm and their respective weights 0.34, 0.33 and 0.33. The diffraction efficiency of a grating optimized at these three blaze wavelengths and computed by scalar theory is given in Figure 11 in comparison with the two reference curves.

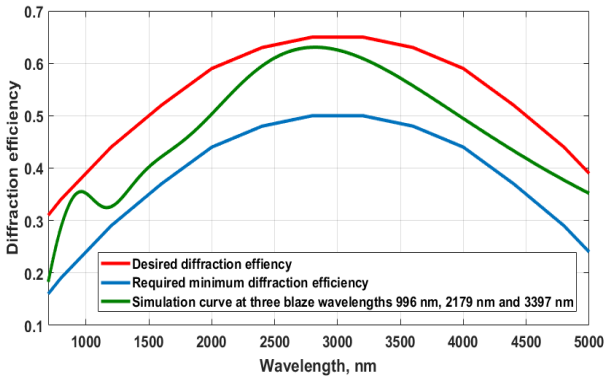

Fig. 11: First order diffraction efficiency for an optimized grating at blaze wavelengths of 996 nm, 2179 nm and 3397 nm, obtained by scalar theory using the ideal profile and compared to the reference curves.

Figure 11 shows that the simulation curve of the optimized grating at three blaze wavelengths of 996 nm, 2179 nm and 3397 nm is not consistent with the desired curve but is well within the range of required diffraction efficiency. The simulation curve is below the desired curve with a surface deficit of 287 AU, which represents a relative difference deficit of 12.16%. The simulation curve is above the required minimum curve with a surplus of 358 AU which represents a relative difference surplus of 20.87%.

Even if the solution is acceptable to the extent that the simulation curve is between the two reference curves, let's see if a solution at four blaze wavelengths can improve the results.

4. Grating solution at four blaze wavelengths

The previous result is consistent. With only three blazes, the simulation curve is well above the required minimum curve (20.87% surplus in relative difference) but slightly below the desired curve (12.16% deficit in relative difference). As in the previous cases, the system to be solved will have 8 variables:
four blaze wavelengths x (1), x (2), x (3) and x (4) and their respective weights x (5), x (6), x (7) and x (8) . Therefore, the initial vector x0 will have 8 components. The solution is
valid if the weights are positive and their sum equal to one. For any initial vector x0, the solution of the system is x = [921; 1669; 2607; 3563; 0.25, 0.25, 0.25, 0.25]. These are the four blaze wavelengths 921 nm, 1669 nm; 2607 nm and 3583 nm and their identical weight 0.25. The diffraction efficiency of an optimized grating at these four blaze wavelengths is given in Figure 12 in comparison with the reference curves.

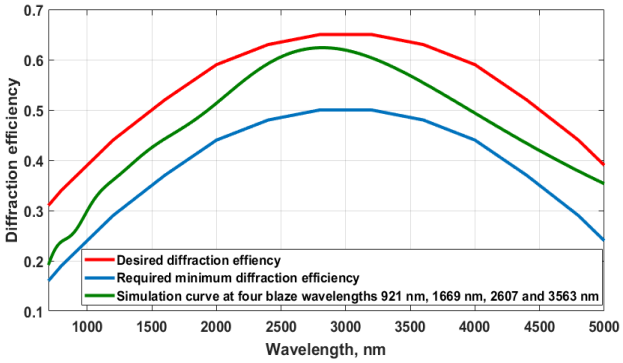

Fig. 12: First-order diffraction efficiency for an optimized grating at four blaze wavelengths of 921 nm, 1669 nm, 2607 nm and 3563 nm, obtained by scalar theory using the ideal profile and compared to the reference curves.

The simulation curve is below the desired curve with a surface deficit of 291AU, which represents a relative difference deficit of 12.33%. The simulation curve is above the required minimum curve with a surface surplus of 354 AU which represents a relative difference surplus of 20.65%. If we compare this solution to the solution with three blaze wavelengths, there is no improvement over the previous solution.

5. Grating solution at five blaze wavelengths

The previous results show that we do not have a simulation curve in agreement with the desired curve, so we see now if a solution with five blaze wavelengths can solve this problem. The system of equations will have 10 unknowns: the five blaze wavelengths and their respective weights. According to the initial vector used, the system admits two types of solution: a solution whose five blaze wavelengths are different and two solutions whose two blaze wavelengths are identical, which amounts to the solution with four blaze wavelengths and they are not better than the solution in the previous section. The only valid solution is x = [903; 1573; 2328; 3022; 3673; 0.23; 0.22; 0.19; 0.18; 0.18] for an initial vector x0 = [900; 1250; 1600; 1950; 2300; 0.1; 0.1; 0.2 0.3, 0.3] for example. The diffraction efficiency of a grating optimized at these five wavelengths is given in Figure 13 in comparison with the reference curves.

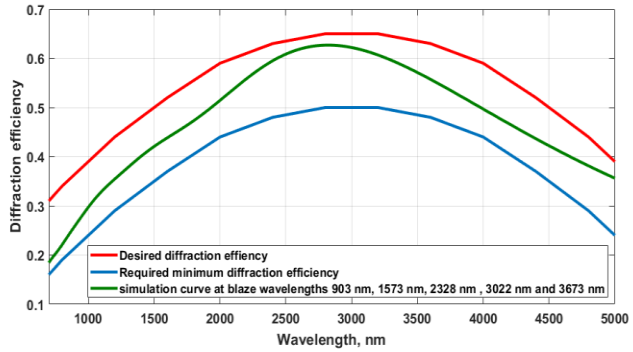

Fig. 13: First order diffraction efficiency for an optimized grating at five blaze wavelengths of 903 nm, 1573 nm, 2328 nm, 3022 nm and 3673 nm obtained by the scalar theory using the ideal profile and compared to the reference curves.

The simulation curve is below the desired curve with a surface deficit of 288 AU, which represents a relative difference deficit of 12.20%. The simulation curve is above the required minimum curve with a surplus of 357 AU which represents a relative difference surplus of 20.81%. This solution is better than the solution with four blaze wavelengths but the solution with three blazes remains the best in that its simulation curve is closer to the desired curve. The question that can be asked now is whether there is a solution capable of producing a curve in accordance with the desired curve. The answer is no because for N = 6, the solution of the system is such that each time one has two identical wavelengths which amounts to a solution with five blazes wavelengths that does not improve the results already found. It is the same for N greater than 6: Each time the solution is such that we have five blaze wavelengths by equality of the blaze wavelengths found, two by two and / or even three.

6. CONCLUSION

From the previous results, there are three solutions in the range of diffraction efficiency desired namely solutions with three (3), four (4) and five (5) blaze wavelengths. The solution at three blaze wavelengths is better because its simulation curve is closer to the desired curve than to the other two. Indeed this solution has a 12.16% deficit in relative difference compared to the desired curve against 12.33% for 4 blaze wavelengths and 12.20% for 5 blaze wavelengths. In addition, having a solution with few blaze wavelengths offers a non-negligible optical advantage. This is the solution for this problem.

G. Study of the impact of realistic profiles on diffraction efficiency and polarization sensitivity

1. Diffraction efficiency

We used scalar theory to determine the number of blaze wavelengths and their weights to obtain a grating with a diffraction efficiency corresponding to the reference curves. The preceding results show that the three-blaze wavelengths solution is the best. We will now use the rigorous theory represented by PCGrate software, the only tool capable of simulating realistic profiles, to study the impact of these profiles on diffraction efficiency and polarization sensitivity. We have constructed these realistic profiles, corresponding to the three blaze wavelengths of 996 nm, 2179 nm and 3397 nm, in the image of Figures 7. The diffraction efficiency of the grating with these ideal and realistic profiles is calculated using the rigorous theory represented by the PCGrate software. Figure 14 shows the diffraction efficiency of the grating optimized at these three wavelengths and computed by the rigorous theory using ideal profiles in comparison with the required minimum curve. There is a great similarity between the diffraction efficiency curve given by the scalar theory and the diffraction efficiency curves given by the rigorous theory especially that of the TM polarized light.

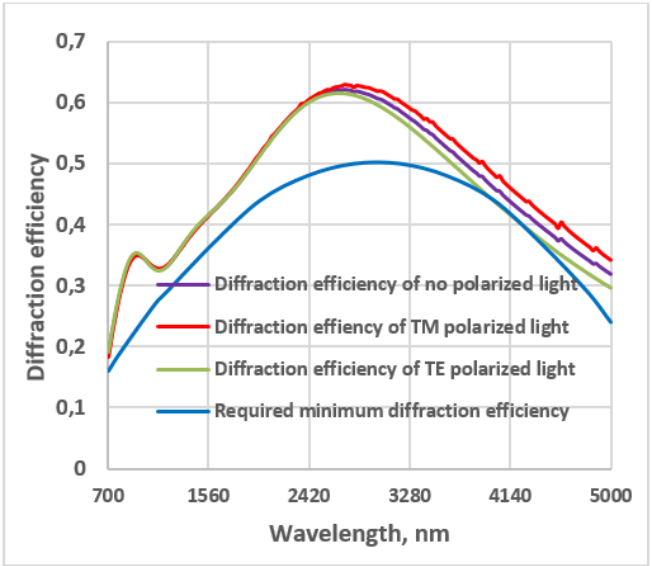

Fig. 14: First-order diffraction efficiency for an optimized grating at blaze wavelengths of 996 nm, 2179 nm and 3397 nm obtained by the rigorous theory PCGrate using the ideal profile with the parameters given in Table 1.

After having constructed the profiles corresponding to these blaze wavelengths as in figures 7, we have simulated these profiles by the rigorous theory to see their impact on diffraction efficiency and polarization sensitivity. Figure 15 gives the diffraction efficiency with the less rounded profiles. The constant is that the maximum efficiency decreases with a

small shift of the curves to the left which results in the decrease of the efficiency in the longest wavelengths and an increase in the smaller wavelengths. Physically this is due to the fact that the depth of the grooves and the period of the deformed profiles decrease slightly compared to the ideal profile. To confirm the rule, we will consider a more rounded profile to see the behavior of the diffraction efficiency curves. The diffraction efficiency of the grating with more rounded profiles is given by Figure 16.

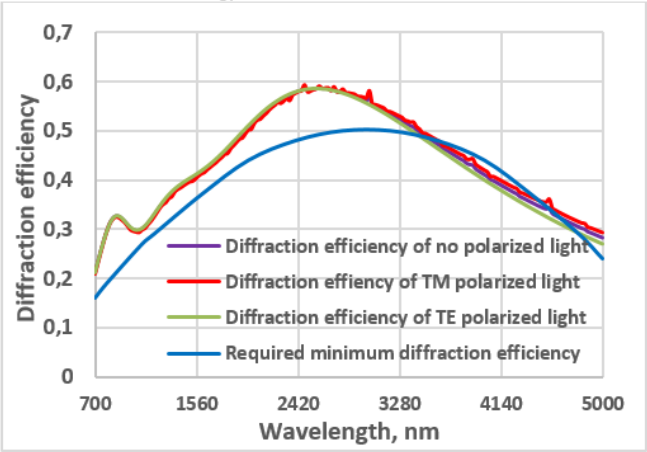

Fig. 15: First order diffraction efficiency for an optimized grating at blaze wavelengths of 996 nm, 2179 nm and 3397 nm obtained by the rigorous PCGrate theory using the less rounded profile with the parameters given in Table 1.

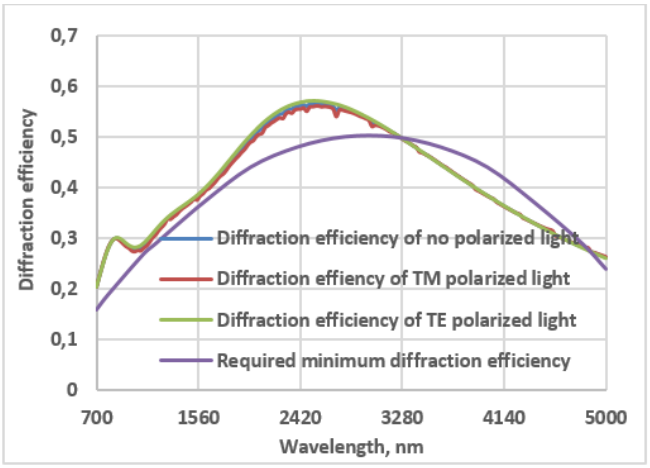

Fig. 16: First order diffraction efficiency for an optimized grating at blaze wavelengths of 996 nm, 2179 nm and 3397 nm obtained by the rigorous theory PCGrate using the more rounded profile with the parameters given in Table 1.

We note that the curves collapse without moving to the left. What is the difference between the two profiles given in Figure 7? They are flattened at the same level at the top but the difference resides in the rounded dimensions of the bottom of the grooves, the more rounded having a bottom rounded on a large radius which has an impact on the real period and depth of the grooves. The conclusion is that the flattened form moves the curves to the left while the rounded shape decrease the diffraction efficiency.

Conclusion

Comparing the ideal and realistic profiles, we note a decrease in efficiency of about 6% from the ideal profile to the more rounded profile. The cause of these changes is the decrease in height and the variation of the real period of the rounded profiles. These deformations therefore result in a decrease in the maximum efficiency of 6%. It is not insignificant and these deformations have to be considered by the manufacturers of grating.

2. Polarization sensitivity

An important drawback when using grating as dispersive element is the relatively large polarization sensitivity i.e. the diffraction efficiency is different for TM and TE polarization. This difference depends on the incidence angle, wavelength and spatial frequency of the grating. The polarization sensitivity of the grating can be studied with the rigorous theory. The equation 9 calculates that dependency as the contrast or degree of polarization:

$$\frac{(\eta_{TE} - \eta_{TM})}{(\eta_{TE} + \eta_{TM})} \qquad (9)$$

Where η_{TE} and η_{TM} are respectively the diffraction efficiencies for TE and TM polarized light.

The polarization dependency of this multi-blazed grating can be deduced from the curves of figures 14, 15 and 16. Figure 17 depicts that dependency as the contrast or degree of polarization for ideal and realistic profiles. In the case of the Chandrayaan 2 hyperspectral imager, the polarization contrast of the grating should remain below 5%. This requirement is met over almost the whole spectral band by the realistic profiles and more than 80% of the band by the ideal profile.

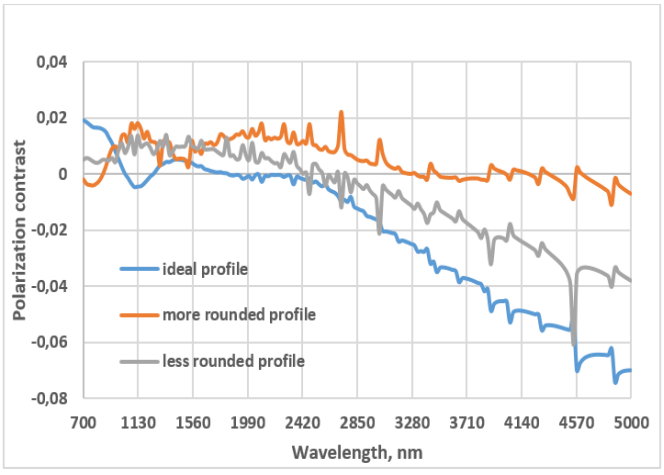

Fig. 17: First-order polarization contrast of an optimized grating at three blaze wavelengths of 996 nm, 2179 nm and 3397 nm blaze based on rigorous theory using ideal and realistic profiles.

H. Diffraction efficiency as a function of incidence angle

Since the multi-blaze grating is convex, the incidence angle of an almost collimated wavefront varies along its surface. For an incidence of 27.12 degrees at the grating center, the incidence angles at left and right ends are respectively 15.04 and 39.20 degrees.

Consequently, the diffraction efficiency of multi-blaze grating with ideal profile as a function of the incidence angle is studied below. The simulation is performed at a

wavelength of 2277 nm. The diffraction efficiency varies from 8% passing from the left (15.04 degrees) end to the right end (39.20 degrees) as shown on figure 18.

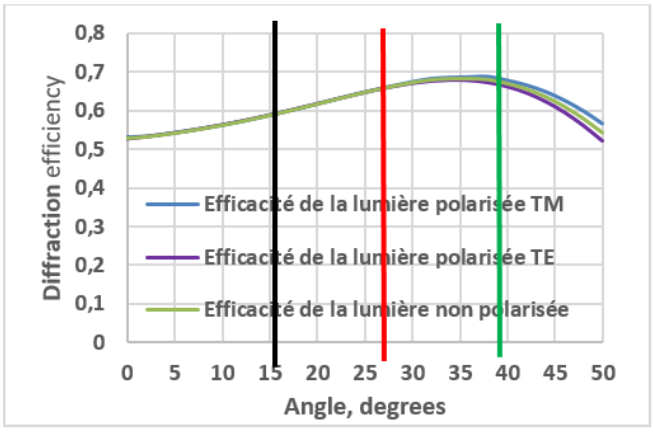

Fig. 18: Diffraction efficiency of optimized grating at three blaze wavelengths, as a function of incidence angle, given by rigorous theory using the ideal profile. The red line indicates the ideal incidence angle (27.12 degrees). The black and green lines indicate respectively the incidence angles at left (15.04 degrees) and right (39.19 degrees) edges of the grating.

The polarization contrast as a function of the incidence angle is given by the figure 19.

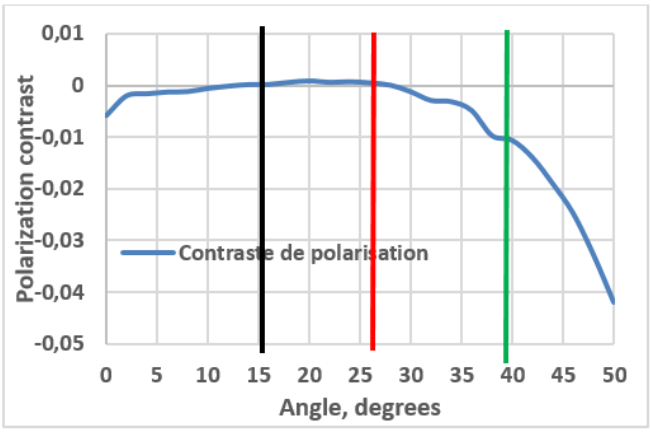

Fig. 19: Polarization contrast of the +1st diffraction order for a multi-blazed grating, as function of incidence angle, based on rigorous theory using ideal profile. The red line indicates the ideal incidence angle (27.12 degrees). The black and green lines indicate respectively the incidence angles at left (15.04 degrees) and right (39.19 degrees) edges of the grating.

As can be seen in Figure 19, the polarization contrast is well below 5% within the limits of use.

VI. Conclusion

The results obtained with single blaze have shown that such diffraction grating cannot cover a spectral range from 0.7 microns to 5 microns with the required diffraction efficiency. Consequently, we proposed a method based on the resolution of a system of nonlinear equations by the function matlab *fsolve*. This method allowed us to move to an optimized grating with 9 blaze wavelengths (in the previous publication) to an optimized grating with 3 blaze wavelengths which offers a considerable optical and manufacturing advantage. These three blaze wavelengths are 996 nm, 2179 nm and 3397 nm and their respective weights 0.34, 0.33 and 0.33. The calculation of the diffraction efficiency using both rigorous and scalar theories has shown that such conception is covering the given spectral band with efficiency matching the required specifications. Unfortunately the diffraction gratings exhibit a non-negligible sensitivity to polarization. We also showed the impact of a rounded profile as encountered with practical manufacturing techniques: the diffraction efficiency decreases with rounded profiles but the polarization sensitivity is also reduced especially in the mid infrared. We also calculated the degree of polarization of multi-blaze depending on the angle of incidence for a wavelength of 2277 nm. The results show that when the angle of incidence remains inside the working limits, the polarization contrast remains low.

REFERENCES

[1] J. R. Schott, *Remote sensing: the image chain approach*. Oxford University Press, Oxford, New York, 2007.

[2] M. T. Eisman, *Hyperspectral Remonte Sensing*, vol. PM210. Bellingham, Washington 98227-0010 USA: SPIE press, 2012.

[3] Indian Space Research Organisation, "Chandrayaan - 2." [Online]. Available: http://www.isro.gov.in/chandrayaan-2.

[4] B. SABUSHIMIKE, G. HORUGAVYE, P. PIRON, J. F. Jamoye, V. Moreau, and S. HABRAKEN, "Design and Modelization of a Convex grating for an Hyperspectral imager of the Chandrayaan 2 instrument for the moon probe in the infrared," *Int. J. Latest Res. Sci. Technol.*, vol. 5, no. 2, p. 6, 2016.

[5] V. Moreau, C. Declercq, J.-F. Jamoye, and A. Z. Marchi, "Free-Form Diffraction Grating for Hyperspectral Imager," *4S Symposium 2014*, Liège, pp. 1–9, 2014.

[6] J. F. Silny and T. G. Chrien, "Large format imaging spectrometers for future hyperspectral Landsat mission," *Proc. SPIE, Imaging Spectrom. XVI*, vol. 8158, no. 815803, pp. 1–26, 2011.

[7] P. Mouroulis, R. G. Sellar, D. W. Wilson, J. J. Shea, and R. O. Green, "Optical design of a compact imaging spectrometer for planetary mineralogy," *Proc. SPIE, Opt. Eng.*, vol. 46, pp. 1–9, Jun. 2007.

[8] B. Sang *et al.*, "The EnMAP hyperspectral imaging spectrometer : instrument concept , calibration and technologies," *Proc. SPIE, Imaging Spectrom. XIII*, vol. 7086, no. 708605, pp. 1–15, 2008.

[9] M. Barnsley, J. Settle, M. Cutter, D. Lobb, and F. Teston, "The PROBA/CHRIS Mission: A low-cost smallsat for hyperspectral, multi-angle, observations of the Earth surface and atmosphere," *IEEE Trans. Geosci. Remote Sens.*, vol. 42, no. 7, pp. 1512–1520, 2004.

[10] C. Palmer, *DIFFRACTION GRATING HANDBOOK*, Sixth edit. New york: Richardson Grating Laboratory, 2005.

[11] International Intellectual Group, "PURPOSES AND TASKS." [Online]. Available: www.iigrate.com.

[12] J. Francés *et al.*, "Comparison of simplified theories in the analysis of the diffraction efficiency in surface-relief gratings," in *Proc. SPIE , Optical Modelling and Design II*, 2012, vol. 8429, pp. 1–10.

[13] V. Raulot, "Méthodes de conception et de fabrication de dispositifs imageurs en optique diffractive à structures sub- longueur d ' onde," Thesis presented for obtaining the degree of Doctor of Engineering Sciences, University of Strasbourg, 2011.

[14] F. Languy, "Achromatization of nonimaging Fresnel lenses for photovoltaic solar concentration using refractive and diffractive patterns," Thesis presented for obtaining the degree of Doctor of Physical Sciences, University of Liège, 2012.

[15] International Intellectual Group, "ACCURATE ELECTROMAGNETIC THEORIES." [Online]. Available: www.PCGrate.com.

[16] P. Mouroulis, D. W. Wilson, R. E. Muller, and P. D. Maker, "New convex grating types for concentric imaging spectrometers .," *Appl. Opt.*, vol. 37, no. 31, pp. 7200–7208, 1998.

[17] I. A. Erteza, "Diffraction Efficiency Analysis for Multi-Level Diffractive Optical Elements," Report of the Sandia National Laboratories for the United states Department of Energy , New Mexico, 1995.

[18] M. Oliva, T. Harzendorf, D. Michaelis, U. D. Zeitner, and a Tünnermann, "Multilevel blazed gratings in resonance domain: an alternative to the classical fabrication approach.," *Opt. Express*, vol. 19, no. 15, pp. 14735–45, Jul. 2011.

[19] E. C. ép. Neiss, “Mise en forme de faisceaux de lasers de puissance dans le proche infrarouge par éléments diffractifs,” Thesis presented for obtaining the degree of Doctor of Engineering Sciences, Louis Pasteur University- Strasbourg I, 2008.
[20] B. SABUSHIMIKE, “Optimization of a multiblaze grating in reflection using free-form profile,” vol. 57, no. 19, 2018.
[21] MathWorks, “fsolve: Functions (optimization toolbox).” MathWorks, 2008.
[22] C. Voglis and I. E. Lagaris, “A Rectangular Trust Region Dogleg Approach for Unconstrained and Bound Constrained Nonlinear Optimization,” in *WSEAS International Conference on Applied Mathematics*, 2004, p. 7.
[23] H. P. Gavin, “The Levenberg-Marquardt method for nonlinear least squares curve-fitting problems,” Department of Civil and Environmental Engineering, Duke University, Durham, NC, USA, 2017.
[24] T. F. Coleman and L. Yuying, “An Interior Trust Region Approach for Nonlinear Minimization Subject to Bounds-1.pdf,” *Siam J. Optim.*, vol. 6, no. 2, p. 28, 1996.
[25] T. F. Coleman and L. Yuying, “On the Convergence of Interior-Reflective Newton Methods for Nonlinear Minimization Subject to Bounds,” *Math. Program.*, vol. 67, no. 2, p. 36, 1994.